8th International Symposium on Magnetic Bearing
August 26-28, 2002, Mito, Japan

ANALYSIS OF A PM HOMOPOLAR TYPE SELF-BEARING STEPPER MOTOR

Daegon Kim
Dept. of Mechanical Eng., KAIST, Taejon, 305-701, Korea
daegonkim@kaist.ac.kr
Kyungwoong Kim
Dept. of Mechanical Eng., KAIST, Taejon, 305-701, Korea
taeho@kaist.ac.kr

ABSTRACT
In this paper the analysis of a permanent magnet (PM) homopolar type self-bearing stepper motor is presented. The self-bearing stepper motor actuator is used for both motor and bearing functionality without any redundant coil windings or redundant electromagnets. The simple example with a cylindrical shape PM is shown. A design of slot type stator and rotor model for small step angle and its analysis are described. Permeance model with PM is used to estimate the air gap flux. Maxwell force production for motor and bearing functionality is developed from the magnetic field energy. A current generation method to minimize energy losses for both motor and bearing functionality is shown in this paper.

INTRODUCTION
Magnetic bearings [1] have been used in the field of high speed and precision electromagnetic actuators due to the non-contact and feedback capabilities. Because the principle of motors and magnetic bearing are very similar, self bearing motors (also termed bearingless motors and integrated motor bearings), which combine motor and magnetic bearing functionality into a single magnetic actuator to perform both radial force and torque production, have been developed. These self-bearing motors offer the advantages of low weight, reduced size, and more.

A stepper motor is an electrical motor that converts a digital input into a mechanical motion using DC power supply, and is used in over 40% of the motor industry. Speed and position control of stepper motors are performed with switching signals of ICs or a microprocessor without any feedback loop.

A design of self-bearing stepper motor using redundant coil windings for bearing functionality was proposed by Higuchi [2]. This design leads to use separate driver for bearing functionality therefore, the size and weight of total system cannot be reduced.

In this paper the analysis of a permanent magnet (PM) homopolar type self-bearing stepper motor without any redundant coil windings or redundant electromagnets is presented. The motor driver is used to drive both stepper motor and magnetic bearings. A design of slot type stator and rotor model including PM and its analysis are described. Permeance model with PM is used to calculate the air gap flux. Maxwell force production for motor and bearing functionality is developed from the magnetic field energy. A current generation method for both motor and bearing functionality is shown in this paper.

This design also has the advantages of magnetic suspension technology. Besides, this design has more advantages to compare with the former self-bearing motor using redundant coil windings or redundant electromagnets;

- To conserve the stepper motor characteristics after conversion to self-bearing stepper motor;
- To reduce size and weight more compared to the former self-bearing motor designs;
- More simple control circuit;
- Minimum net power loss because of no additional current for bearing functionality.

This new actuator can replace with most of stepper motor applications, and especially can be applied to;

- computer peripherals: hard disk drive, printer;
- office equipment: copier, fax machine;
- MEM's actuators: pump, compressor, centrifuge;
- space based actuators: satellite gimbal and flywheel, high precision tracking and positioning system;
- precision control actuators: x-y table, robot actuator, semiconductor equipments;
- military purpose actuators: missile tracking system;
- medical instruments: artificial heart pump.

ANALYSIS
The stepper motor is an electrical motor, which converts

a digital electric input into a mechanical motion. The characteristics of the stepper motor are the step-by-step turning, which is made up from a specified number of steps. Self-bearing stepper motors also operate with the same manner.

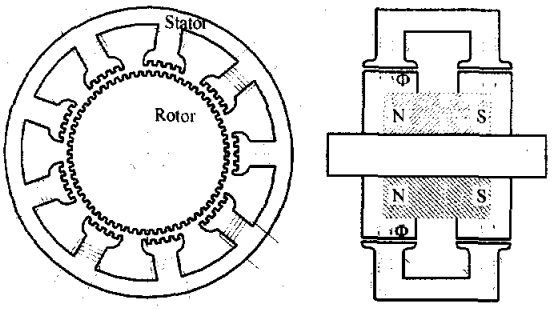

(a) Front view (b) Side view

FIGURE 1: Schematics of PM homopolar type self-bearing stepper motor

Figure 1 shows the layout of the PM toothed type self-bearing stepper motor consisting 60 teeth on the rotor and 9 electromagnetic poles with 5 teeth each. A cylindrical PM is mounted as shown in figure 1(b), therefore, flux flows axially. In the conventional stepper motors the coil windings in the same phase are connected serially, however in the proposed self bearing stepper motor, the coil connections for same phases are cut off to drive each coil independently. To grant self bearing functionality into conventional stepper motors, there are some issues to be solved; first, the overlapped length change between stator and rotor teeth; second, phase commutation for rotation; third, independent motor torque and bearing forces production for easy applications. These issues can be solved with both hardware and software approach.

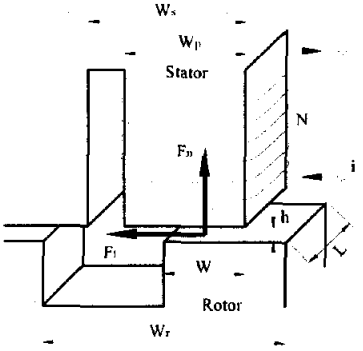

FIGURE 2: Force at overlapped area

Figure 2 shows a single electromagnet of the actuator, and unrolled as an approximation to the true arc geometry. The stator and rotor have axial length, L, stator pitch, W_s, rotor pitch, W_r, radial length of electromagnetic pole, W_p, air gap, h, and overlapped length, W. In general stepper motors the normal directional forces are restricted by mechanical bearings, and only the tangential directional forces are used to produce motor torque. However, in the proposed self-bearing stepper motors the normal directional forces are used to support the rotor, and tangential directional forces are also used to generate motor torque. The simplest equation of Maxwell type electromagnetic force is based on the field energy method with the infinite permeable core assumption. Using the field energy method with the infinite permeable core assumption, the normal and tangential directional forces are expressed as:

$$F_n = \frac{LWB_g^2}{\mu_0} \tag{1}$$

$$F_t = \frac{LhB_g^2}{\mu_0} \tag{2}$$

where μ_0 is the permeability of free space and B_g is the air gap flux density. As mentioned before, the overlapped length, W, is changed with rotor rotation, and air gap, h, is dependent upon the rotor position. Air gap flux is also dependent upon both overlapped length and air gap. To estimate the exact permeance is difficult, because flux does not flow straight across near the edge of the blocks. In this paper straight line, circular arc permeance model is used to calculate air gap flux and is derived by [3, 4]:

$$P = \frac{\mu_0 LW}{k_c h} \tag{3}$$

where k_c is a fringing flux compensation factor similar to Carter's coefficient as:

$$k_c = \left(1 + \frac{2h}{\pi L}\ln\left(1+\frac{\pi r_m}{h}\right) + \frac{4h}{\pi W}\ln\left(1+\frac{\pi r_m}{2h}\right)\right)^{-1} \quad \text{for } r_m \le r_{(W_p - W)} \tag{4a}$$

$$k_c = \left(1 + \frac{2h}{\pi L}\ln\left(1+\frac{\pi r_m}{h}\right) + \frac{4h}{\pi W}\ln\left(1+\frac{\pi r_m}{2h}\right) + \frac{2h}{\pi W}\ln\left(\frac{h+\pi r_m - \pi(W_p - W)/2}{h+\pi(W_p - W)/2}\right)\right)^{-1} \quad \text{for } r_m > r_{(W_p - W)} \tag{4b}$$

The fringing flux compensation factor is fluctuated due to the overlapped length and air gap.

Assuming that the permeability of the core is much greater than that of the surrounding air, the magnetic field is essentially confined to the core, except the air gap. Then, figure 1(b) can be approximated with magnetic circuit analysis. Given the air gap flux and ideal permeance in the previous equations, air gap flux density is calculated by:

$$B_g = \frac{\mu_0\left(2Ni + B_r l_m / \mu_0\mu_r\right)}{\left(2k_c h + Ll_m W / \mu_r A_m\right)} \tag{5}$$

where B_r is the remanence flux density, μ_r is the recoil permeability, A_m is the cross sectional area of the PM face in the direction of magnetization, and l_m is the length of the PM. Substituting eq(5) into eq(1) and (2), normal and tangential forces for one slot can be calculated by:

$$F_{nj} = \frac{\mu_0 S_n N_n LW \left(2Ni + {B_r l_m}/{\mu_0 \mu_r}\right)^2}{\left(2k_c h + {Ll_m W}/{\mu_r A_m}\right)^2} \quad (6)$$

$$F_{tsf} = \frac{\mu_0 S_n N_n Lh \left(2Ni + {B_r l_m}/{\mu_0 \mu_r}\right)^2}{\left(2k_c h + {Ll_m W}/{\mu_r A_m}\right)^2} \quad (7)$$

where N_n is slot number, S_n is the tooth coefficient $S_n<1$ and depends upon the geometry of the rotor and stator teeth, and computed by:

$$S_{n,odd} = \frac{1}{N_n}\left(1 + \sum_{n=1}^{(N_n-1)/2} \cos\left(\frac{2\pi n}{N_r}\right)\right)$$
$$S_{n,even} = \frac{2}{N_n}\sum_{n=1}^{N_n/2} \cos\left(\frac{2\pi(2n-1)}{N_r}\right) \quad (8)$$

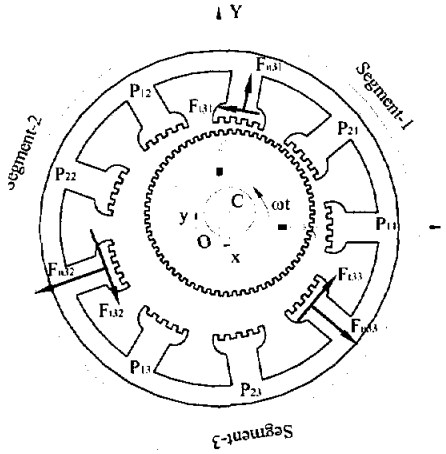

FIGURE 3: Air gap and force production at phase III excitation

Figure 3 shows the relationship between air gap and force production, when the electromagnets in phase III are excited. The air gap of each electromagnets are computed by:

$$h_{jk} = h_s - x\cos(\theta_{jk}) - y\sin(\theta_{jk}) \quad (9)$$

where h_s is the radial air gap with the rotor in a centered position and θ_{jk} is the angle of geometric center at each electromagnetic pole. This angle depends upon the number of segments and electromagnetic poles as:

$$\theta_{jk} = \frac{2\pi}{N_k}(k-1) + \frac{2\pi}{N_s}(j-1) \quad (10)$$

Control current selection must be done with respect to two control currents, i_x, i_y, and torque current, i_t. They correspond to the bearing forces and motor torque in each direction. In this paper, the torque current is considered as constant, therefore, two currents i_x and i_y are being used to generate two directional bearing forces. There are many different current relationships to choose from. Using the air gap geometric relationship, the simplest current relationships can be estimated as:

$$i_{jk} = i_t + i_x\cos(\theta_{jk}) + i_y\sin(\theta_{jk}) \quad (11)$$

For k sets of control current, the summation of control currents $\sum i_x\cos(\theta_{jk}) + i_y\sin(\theta_{jk})$ in this equation is always zero, therefore no additional current for bearing functionality is necessarily. This leads that the power loss can be minimized. Substituting eqs (9) and (11) into equations (6) and (7), and linearizing these equations using Taylor series expansion, the following x and y directional force equations when j^{th} phase is being driven:

$$F_{njk}(\omega t) = F_{n0} + K_{nq}\cos(\theta_{jk})x + K_{nq}\sin(\theta_{jk})y + K_{ni}\cos(\theta_{jk})i_x + K_{ni}\sin(\theta_{jk})i_y \quad (12)$$

$$F_{tjk}(\omega t) = F_{t0} + K_{tq}\cos(\theta_{jk})x + K_{tq}\sin(\theta_{jk})y + K_{ti}\cos(\theta_{jk})i_x + K_{ti}\sin(\theta_{jk})i_y \quad (13)$$

where each parameter is calculated with following equations:

$$F_{n0} = \frac{\mu_0 S_n N_n LW \left(2Ni_t + {B_r l_m}/{\mu_0 \mu_r}\right)^2}{\left(2k_c h_s + {Ll_m W}/{\mu_r A_m}\right)^2} \quad (14)$$

$$k_{nq} = \frac{4\mu_0 S_n N_n Lk_c W \left(2Ni_t + {B_r l_m}/{\mu_0 \mu_r}\right)^2}{\left(2k_c h_s + {Ll_m W}/{\mu_r A_m}\right)^3} \quad (15)$$

$$k_{ni} = \frac{4\mu_0 S_n N_n NLW \left(2Ni_t + {B_r l_m}/{\mu_0 \mu_r}\right)}{\left(2k_c h_s + {Ll_m W}/{\mu_r A_m}\right)^2} \quad (16)$$

$$F_{t0} = \frac{\mu_0 S_n N_n Lh_s \left(2Ni_t + {B_r l_m}/{\mu_0 \mu_r}\right)^2}{\left(2k_c h_s + {Ll_m W}/{\mu_r A_m}\right)^2} \quad (17)$$

$$k_{tq} = \frac{\mu_0 S_n N_n L\left(2k_c h_s - {Ll_m W}/{\mu_r A_m}\right)\left(2Ni_t + {B_r l_m}/{\mu_0 \mu_r}\right)^2}{\left(2k_c h_s + {Ll_m W}/{\mu_r A_m}\right)^3} \quad (18)$$

$$k_{ii} = \frac{4\mu_0 S_n N_n N L h_s \left(2Ni_i + B_r l_m / \mu_0 \mu_r\right)}{\left(2k_c h_s + L l_m W / \mu_r A_m\right)^2} \quad (19)$$

Similarly, torque produced by the actuator is computed using:

$$T = \frac{\mu_0 S_n N_n N_k r L h_s \left(2Ni_i + B_r l_m / \mu_0 \mu_r\right)^2}{\left(2k_c h_s + L l_m W / \mu_r A_m\right)^2} \quad (20)$$

From equations (12) and (13) x and y directional forces are calculated as:

$$F_{xj}(\omega t) = \sum_{k=1}^{N_k}\left[F_{mjk}(\omega t)\cos(\theta_{jk}) - F_{ijk}(\omega t)\sin(\theta_{jk})\right] \quad (21)$$

$$F_{yj}(\omega t) = \sum_{k=1}^{N_k}\left[F_{mjk}(\omega t)\sin(\theta_{jk}) + F_{ijk}(\omega t)\cos(\theta_{jk})\right] \quad (22)$$

These equations can be rearranged as:

$$F_{xj}(\omega t) = K_q x - K_{qc} y + K_i i_x - K_{ic} i_y \quad (23)$$

$$F_{yj}(\omega t) = K_{qc} x + K_q y + K_{ic} i_x + K_i i_y \quad (24)$$

where K_q and K_{qc} is the displacement stiffness coefficient, K_i and K_{ic} is the current stiffness coefficient, and are calculated by:

$$K_q = \frac{N_k}{2} k_{nq}, \quad K_{qc} = \frac{N_k}{2} k_{tq} \quad (25)$$

$$K_i = \frac{N_k}{2} k_{ni}, \quad K_{ic} = \frac{N_k}{2} k_{ti} \quad (26)$$

The dynamic equation of self bearing stepper motor can be constructed as:

$$\dot{\mathbf{x}} = \mathbf{A}\mathbf{x} + \mathbf{B}\mathbf{u} \quad (27)$$

$$\mathbf{A} = \begin{bmatrix} 0 & 0 & 1 & 0 \\ 0 & 0 & 0 & 1 \\ k_q/m & -k_{qc}/m & 0 & 0 \\ k_{qc}/m & k_q/m & 0 & 0 \end{bmatrix} \quad (28)$$

$$\mathbf{B} = \begin{bmatrix} k_i/m & -k_{ic}/m \\ k_{ic}/m & k_i/m \end{bmatrix} \quad (29)$$

where the state vector is $\mathbf{x} = \{x \quad y \quad \dot{x} \quad \dot{y}\}^T$, control vector is $u = \{i_x \quad i_y\}^T$, and m is rotor mass.

Current regulator generates k sets of supplying currents for the phase excitation, which is simultaneously switched by the step motor controller. In practical application, three kinds of feedback control loops can be achieved for bearing control current generation, according to the position of the current regulator; between sensor transducer and reference comparator, between bearing controller and power amplifier, and between power amplifier and actuator coil. The number of bearing controllers and power amplifiers needed is determined by the position of the displacement compensator; k sets of bearing controllers and power amplifiers for the first case, two bearing controllers and k power amplifiers for the second case, and two sets of bearing controllers and two sets of power amplifiers for the third case are required. Therefore the third case is better than other cases in the constructional viewpoint. However, in this case some large size electric elements for high power summing junctions are required. In the signal generation viewpoint, the first case may be the best way to get any proper control signals, which we are expecting, because each exciting pole signal will be controlled independently; whereas in the second and third case, the supplying currents will be approximated using X and Y directional controlled signals, which may result in the other vibration source. Selection of the position of displacement compensation depends upon where this actuator will be applied. The important thing is that the displacement compensator will be switched with the step motor driving switch at the same time.

The sensor detects the geometric deviation of the rotor and the signal is used to construct an error signal, which is fed into controllers and power amplifiers and generates the control currents, i_x and i_y. These control currents are regulated at the current regurator according to the phase excitation. They then generate k supplying currents for each segment coil.

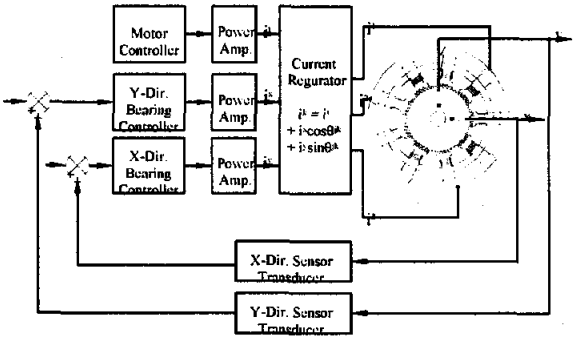

FIGURE 4: Feedback loop for self bearing stepper motors

SIMULATION RESULTS

To illustrate the analysis and control algorithm of the PM homopolar type self-bearing stepper motor, a

simple model is used as; 3-phase, 9 electromagnetic pole pairs, 5 teeth on each magnetic pole, and 60 teeth on the rotor. The properties of this model are listed in Table 1, which are used in a simulation of the motor response to a rotating unbalance, 1μm, and constant angular velocity, $1s^{-1}$. Next step velocity and displacement of the rotor are calculated using Adams method..

TABLE 1: Construction of the PM Homopolar type self-bearing step motor

Property	Symbol	Value
Rotor mass	m	1.0Kg
Rotor radius	R	0.02m
Axial length of the actuator	L	0.01m
Steady state air gap	h_s	0.0005m
Number of coil turns	N	100
Number of electromagnets	N_s	9
Number of slot per a pole	N_n	5
Number of rotor slot	N_r	60
Remanence flux density	B_r	o.4
Cross sectional area of PM	A_m	$0.0001m^2$
Axial length of PM	l_m	0.01m
Recoil permeability	μ_r	1.1
Motoring current	i_t	2 A
Sensor transducer gain	G_s	5000V/m
Power amplifier gain	G_a	1 A/V
Proportional gain	$G_{px}=G_{py}$	1.0
Derivative gain	$G_{dx}=G_{dy}$	0.0001
Integral gain	$G_{ix}=G_{iy}$	1.0

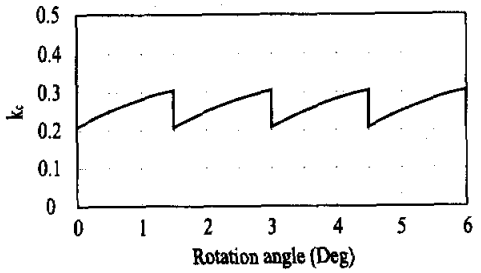

FIGURE 5: Fringing flux compensation factor variation to slot facing area

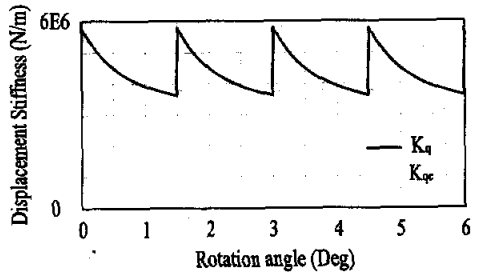

FIGURE 6: Displacement stiffness

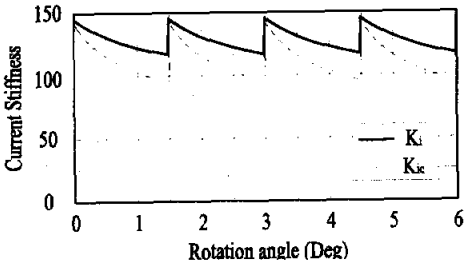

FIGURE 7: Current stiffness

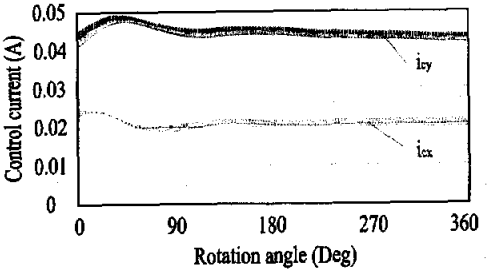

FIGURE 8: Bearing control current under rotating unbalance

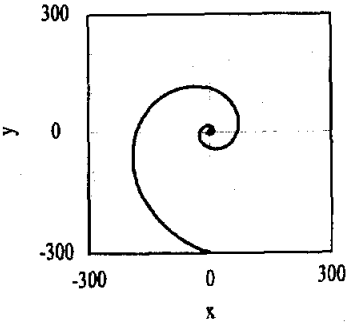

FIGURE 9: Rotor locus during first three revolutions (μm)

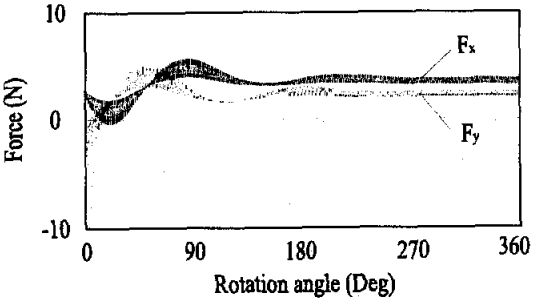

FIGURE 10: Bearing forces under rotating unbalance

Figure 5 shows the fringing flux compensation factor according to the rotor rotation. The extent of the fringing permeance, r_m is commonly chosen to be some multiple of the air gap length beyond 10×h. However, in this analysis, the air gap is larger than the traditional

stepper motor construction, so we chose 5×h. The fringing flux compensation factor is unity when no fringing effect is considered. However, if we consider this effect, fringing flux compensation factor for r_m=5×h is changed from 0.21 to 0.31 according to the overlapped area. This will influence on the system performances so much as shown in following results therefore, the proper modeling and estimation for fringing effect are necessarily.

Figure 6 and figure 7 show the simulated displacement stiffness and current stiffness. Both of the stiffness are changed periodically with the step angle. However, these fluctuation can be reduce or remove using traditional stepper motor excitation method and/or modified active control algorithm.

Figure 8 shows the bearing control current under the unbalance response at transient state. The main oscillation under 90° is to levitate the rotor, and the small variation is due to the overlapped area between stator and rotor.

Figure 9 shows the rotor locus during first three rotation of the rotor. As expected, rotor was levitated independent with motor functionality.

Figure 10 shows the x- and y-directional bearing forces to compensate the rotor position.

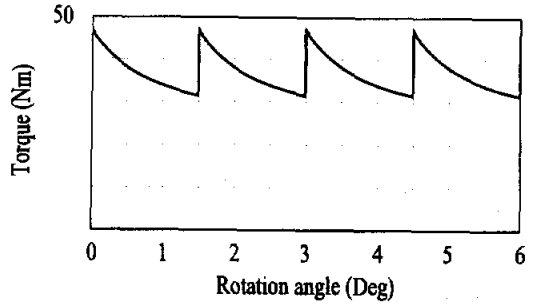

FIGURE 11: *Torque response under rotating unbalance*

Figure 11 shows the torque response. The fluctuation of the torque is due to the change of the overlapped area. This can be overcome with the conventional stepper motor technology to change excitation method and/or to use active control. But, the most important thing in this paper is that the torque characteristic should not change whether the bearing functionality is added in motor functionality or not.

CONCLUSIONS

This paper introduces the principles of motor torque and bearing force of the 3-phase PM homopolar type self-bearing stepper motor, in which the commercially available motor actuator is used for both motor and bearing functionality without any redundant coil windings or redundant electromagnets. The principles of torque and bearing force productions were analyzed. Analysis showed the following: (1) commercially available step motor can be applied to the self bearing stepper motor without any redundant coil windings or electromagnetic poles; (2) energy loss can be minimized due to the proper current generation method; (3) the same torque generation is possible, whether bearing functionality is added or not. From the results the proper modeling and estimation the proper excitation method to reducing the torque and stiffness fluctuation is need. Also, future work will contain experimental results from the prototype self-bearing stepper motor.

REFERENCES

1. Daegon Kim, Kyungwoong Kim, "The Influence of the Machining and Assembling Errors on the Performance of the Shaft Supported by Active Magnetic Bearings", JSME International Journal, Series C, Vol. 41, No. 2, pp. 313-320, Jun. 1998.
2. Higuchi, 1987, "Magnetically Floating Actuator Having Angular Positioning Function," US Patent, No. 4683391.
3. Daegon Kim, "Control of a 3-Phase VM Type Self-Bearing Step Motor", Journal of KSME, Vol. 25, No. 12, pp. 1974-1980, Dec. 2001.
4. Daegon Kim, L. S. Stephens, "Analysis of a 3-Phase VR Type Self-Bearing Step Motor", Proceedings of 6th International Symposium on Magnetic Suspension Technology, pp. 262-265, Oct. 2001.
5. Takashi Kenjo, 1984, "Stepping Motors and Their Microprocessor Controls," Oxford University Press, Oxford.